# Solubilization of *n*-Alkylbenzenes into Gemini Surfactant Micelles in Aqueous Medium

Hiromichi Nakahara, Yui Kojima, Yoshikiyo Moroi, and Osamu Shibata*

Department of Biophysical Chemistry, Faculty of Pharmaceutical Sciences, Nagasaki International University; 2825-7 Huis Ten Bosch, Sasebo, Nagasaki 859-3298, Japan

S *Supporting Information*

ABSTRACT: Solubilization of benzene, toluene, ethylbenzene, *n*-propylbenzene, *n*-butylbenzene, and *n*-pentylbenzene into micelles of decanediyl-1-10-bis-(dimethyltetradecylammonium bromide) (14-10-14,2Br⁻) has been investigated in the temperature range from 288.2 to 308.2 K. The equilibrium concentrations of all the solubilizates are determined spectrophotometrically. The concentration of the solubilizates remains constant below the critical micelle concentration (cmc) and increases linearly with an increase in 14-10-14,2Br⁻ concentration above the cmc. Compared to the mother micelle, the solubilized micelles indicate much larger hydrodynamic diameters, which are determined by dynamic light scattering. Therefore, the Gibbs energy change for the solubilization of *n*-alkylbenzenes has been evaluated by the partitioning of the solubilizates between the aqueous and micellar phases. Furthermore, the enthalpy and entropy changes for the solubilization could be calculated from temperature dependence of the Gibbs energy change. From the thermodynamic parameters, it is found that the solubilization for the present system is entropy-driven and that the location of the solubilizates moves into the inner core of the micelle with an elongation of their alkyl chains. The movement on the location is also supported by the results of absorption spectra, Fourier transform infrared (FTIR) spectra, and two-dimensional nuclear Overhauser effect spectroscopy (2-D NOESY).
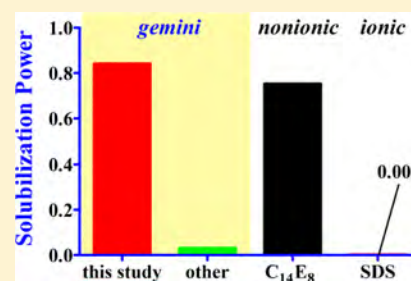
INTRODUCTION

Aqueous solubility of organic substances increases via their incorporation into micelles in surfactant solutions, which results in a thermodynamically stable isotropic solution. The phenomenon is known as solubilization.[1−3] Indeed, solubilization has been applied to a wide variety of scientific fields as well as industrial ones. For practical use and application, a surfactant with low critical micelle concentration (cmc) is often considered to play an efficient role in solubilization. It is well-known that the cmc of nonionic surfactants is much lower compared to that of ionic surfactants. Therefore, nonionic surfactant solutions incorporated by a hydrophobic dye have been investigated from the perspective of solubilization.[4−9] However, a key factor in the solubilization process is apparently not low cmc of the surfactants only. Indeed, it has been reported that a driving force of transfer of solubilizates from bulk to micellar aggregates is completely different between nonionic and ionic surfactants.[6,7,10,11] In this regard, mixed micelles of ionic and nonionic surfactants have been under extensive investigation as a potential solubilizing agent.[12−15]

Gemini or dimeric surfactants, which consist of two hydrophobic chains and two hydrophilic headgroups in a molecule,[16,17] have gained much interest over the past decades due to their much lower cmc (1−2 orders of magnitude lower), superior surface activity, better lime-soap dispersing, more useful viscoelastic property, and better wetting property compared to those for corresponding conventional monomeric surfactants.[18−21] The most studied gemini surfactant with

regard to biological[22−26] and physicochemical properties[27−30] is the cationic type (*m-s-m*,2Br⁻). It has two quaternary ammonium species ($C_mH_{2m+1}N^+(CH_3)_2$) linked covalently by a hydrocarbon spacer ($-C_sH_{2s}-$). The effect of hydrophobic chain length and structure of the spacer on their adsorption and aggregation behavior has been studied in detail.[19−21] To our knowledge, however, there are few reports on the studies of solubilization into gemini-surfactant micelles,[31,32] although the solubilization into the micelles of typical ionic and nonionic surfactants have been extensively investigated in a thermodynamical manner.[4−7,33] As mentioned above, the combination of the much lower cmc and the ionic hydrophilic groups for the gemini surfactants would have a great advantage in solubilization. In this regard, the mechanism of solubilization into gemini-surfactant micelles must be extensively clarified toward practical use in the industrial, medical, pharmaceutical, and cosmetic fields.

In the present study, we report the solubilization of *n*-alkylbenzenes such as benzene, toluene, ethylbenzene, *n*-propylbenzene, *n*-butylbenzene, and *n*-pentylbenzene into 14-10-14,2Br⁻ micelles, which have previously been characterized in the aqueous medium.[34] The solubilization has been performed in the temperature range from 288.2 to 308.2 K with an interval of 10 K in order to clarify the effects of the

benzene rings and of alkyl chain lengths of *n*-alkylbenzenes on the thermodynamic parameters of solubilization. In addition, the size variation of the solubilized micelles or aggregates is elucidated in terms of hydrodynamic diameters derived from dynamic light scattering. The location of the solubilizates in the micelle is also investigated using absorption spectra and Fourier transform infrared (FTIR) spectra as well as two-dimensional nuclear Overhauser effect spectroscopy (2-D NOESY). 2-D NOESY is a powerful technique for examining the spatial interactions in close vicinity (<0.5 nm) between two different components.[35,36] Furthermore, these data are normalized as a solubilization power in order to compare with the ones of other types of surfactants.

■ EXPERIMENTAL SECTION

Materials. Decanediyl-1-10-bis(dimethyltetradecylammonium bromide) (abbr. 14-10-14,2Br⁻) was synthesized via the procedure reported previously.[21] Detailed information on the purification and identification for 14-10-14,2Br⁻ was described elsewhere.[34] Benzene (>99.5%), toluene (99.5%), ethylbenzene (>99.0%), *n*-propylbenzene (>99.0%), and *n*-butylbenzene (>99.0%) were purchased from Tokyo Chemical Industry Co., Ltd. (Tokyo, Japan). *n*-Pentylbenzene (99.0%) was bought from Aldrich (MO, USA). *n*-Dodecane (99%) and deuterium oxide (D₂O, 99.96%) were purchased from Wako Pure Chemical Industries (Osaka, Japan) and Merck KGaA (Darmstadt, Germany), respectively. These reagents were used as received. The water used throughout the present study was thrice-distilled (surface tension = 72.0 mN m⁻¹ at 298.2 K and electrical resistivity = 18 MΩ cm).

Methods. *Solubilization.* The 14-10-14,2Br⁻ solution of nine different concentrations was filtered through a membrane filter of 0.1 μm pore size (Millipore MILLEX VV) to remove dust. Nine surfactant solutions were poured separately into nine photocells, which were then set into the solubilization apparatus. About 30 μL of benzene and toluene was placed on the bottom of a small vessel in the middle of the glass apparatus in order for the maximum absorbance to be less than 0.7. As for the other *n*-alkylbenzenes, 1 mL of liquid solubilizates was dropped inside the middle vessel. The whole glass apparatus with its cover was kept in a thermostat controlled within ±0.1 K at 288.2, 298.2, and 308.2 K for 24−48 h to reach complete solubilization equilibrium, where the nine surfactant solutions were agitated with a rotor in each photocell. Detailed information on the apparatus and the procedures of solubilization is described elsewhere.[6,7,37] The solubilizate concentrations in the surfactant solutions were determined spectrophotometrically with a UV/vis spectrophotometer (V-530, Jasco, Tokyo, Japan) by the optical density of the solutions and the molar extinction coefficient (ε); the ε values at 260 nm were 232, 216, 201, 211, and 222 mol⁻¹ dm³ cm⁻¹ for toluene, ethylbenzene, *n*-propylbenzene, *n*-butylbenzene, and *n*-pentylbenzene, respectively, and the value at 254 nm was 188 mol⁻¹ dm³ cm⁻¹ for benzene.[38−40] The points in the figures are the means ± SD. The set of measurements was repeated five times at least.

Dynamic Light Scattering (DLS). DLS measurements were performed with a Zetasizer Nano-S (Malvern Instrument Ltd., Worcestershire, UK) using a 5 mW He−Ne laser (λ = 633 nm). Prior to the measurement, all surfactant solutions were filtered once through a 0.1 μm pore-size membrane filter. The measurements were carried out at three different temperatures of 288.2, 298.2, and 308.2 ± 0.1 K. The set of measurements were made at least five times at each temperature. The apparent hydrodynamic diameter (d_H) of surfactant micelle was calculated according to the Einstein-Stokes relation:

$$d_H = \frac{k_B T}{3\pi\eta D_0} \tag{1}$$

where D_0 is the diffusion coefficient extrapolated to zero concentration, k_B is the Boltzmann constant, T is the Kelvin temperature, and η is the viscosity of the medium.

Cryogenic Transmission Electron Microscopy (cryo-TEM). The cryo-TEM observation was performed with a Hitachi H-7650 transmission electron microscope with a tungsten filament, operating at 120 kV. To avoid serious damage of the samples by electron beam irradiation, the cryo-TEM observation was performed under a low dose condition (3.0 mA). The direct magnification used here was 15000−20000 times. For the sample preparation, a Leica EM CPC was utilized. First, a drop (∼20 μL) of each sample was mounted on a hydrophilized microgrid (Okenshoji, Tokyo, Japan) supported between vertically hung locking tweezers. Under observation with binoculars in the light, the droplet was carefully absorbed with filter paper until an interference pattern appeared. Once the thin film formed, the tweezers were dropped into a container of liquid ethane which was further chilled with liquid nitrogen. Then, the vitrified sample was swiftly transferred to a Gatan cryo-TEM holder equipped with a Dewar flask for TEM observation.

Fourier Transform Infrared (FTIR) Spectra. FTIR spectra were recorded in transmission mode with a Fourier transform spectrometer (JASCO FT/IR-4200, Tokyo, Japan). The 14-10-14,2Br⁻ solutions at 2.0 mmol dm⁻³ solubilizing *n*-alkylbenzenes or the liquid sample of *n*-dodecane containing appropriate amounts of benzene were loaded into a CaF₂ cell (JASCO) with 0.05 mm path length and analyzed over a range of wavenumbers from 4000 to 400 cm⁻¹ at room temperature (∼298.2 K). Each spectrum was collected under an accumulation of 512 scans at a nominal resolution of 2 cm⁻¹. Pure solvents in the CaF₂ cell were taken as background references before measuring sample spectra.

Nuclear Magnetic Resonance (NMR). NMR experiments were performed using a JNM-AL400 spectrometer (Jeol, Tokyo, Japan). ¹H NMR spectra were acquired at 298.2 K. The stock solutions of 14-10-14,2Br⁻ and *n*-alkylbenzenes were prepared in D₂O. The proper amounts of each mixture were transferred to a 5 mm NMR tube (Wilmad-LabGlass, NJ, USA). Two-dimensional nuclear Overhauser effect spectroscopy (2-D NOESY) experiments were conducted at 298 K with 300 ms mixing time. Each spectrum consisted of 64 scans.

■ RESULTS

Solubility of *n*-Alkylbenzenes. The change in concentration for *n*-alkylbenzenes with 14-10-14,2Br⁻ concentration is shown in Figure 1 (298.2 K) and SI Figure S1 (288.2 and 308.2
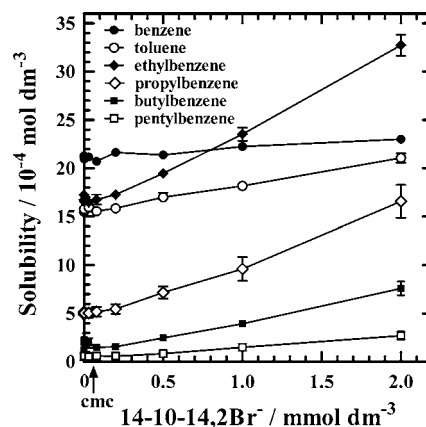
Figure 1. Concentration changes of *n*-alkylbenzenes with 14-10-14,2Br⁻ concentration at 298.2 K.

K). The critical micelle concentration (cmc) of 14-10-14,2Br⁻ was determined previously by the electrical conductivity measurement:[34] 0.0586 (288.2 K), 0.0600 (298.2 K), and 0.104 mmol dm⁻³ (308.2 K). The solubilizate concentrations below the cmc remain almost constant for all the solubilizates (see Figure S2), which indicates the constancy of the chemical potential of solubilizate molecules throughout the phases inside
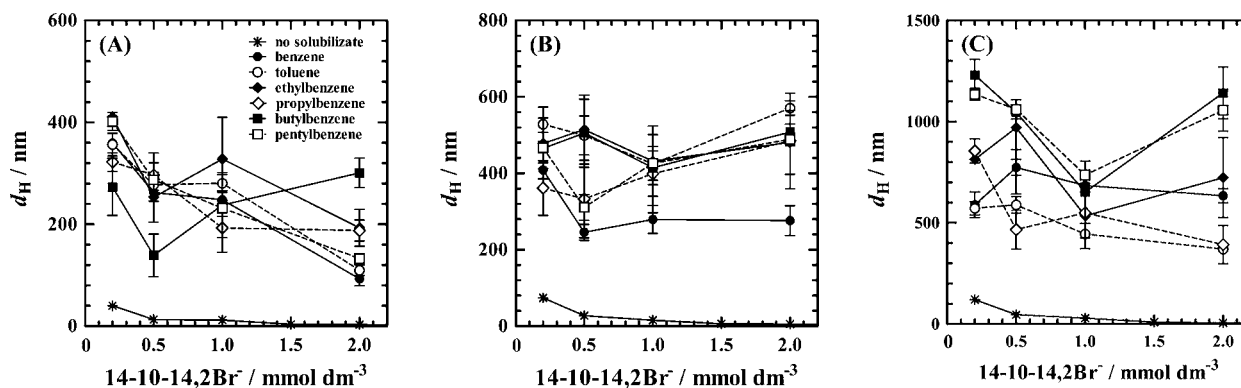
Figure 2. Variation in hydrodynamic diameter (d_H) of the aggregates with 14-10-14,2Br$^-$ concentration at (A) 288.2, (B) 298.2, and (C) 308.2 K.

the glass apparatus. In addition, the aqueous solubilities for the *n*-alkylbenzenes except for benzene and toluene (at 0 mmol dm^{-3} 14-10-14,2Br$^-$ concentration) are almost consistent with the reference values.[41−43] As for the two, the amount placed in the system is controlled as described above. The other concentrations are the equilibrium concentrations, because the solubilizate phase continues to coexist in the system. In addition, the mean value of the solubilizate concentrations below the cmc gives the value of the monomer concentration of the solubilizate in aqueous bulk [R]. An increase in the solubilizate concentration above the cmc is caused by an incorporation of the solubilizates into the micellar aggregates. The concentration of *n*-alkylbenzenes decreases in the order of (benzene > toluene >) ethylbenzene > *n*-propylbenzene > *n*-butylbenzene > *n*-pentylbenzene, which is the same as the decreasing order of aqueous solubility, where (benzene > toluene >) represents the concentration depending on the molar amount of liquid placed inside the apparatus. Namely, the results indicate that the amount solubilized in the aggregates becomes larger for more soluble solubilizate in the aqueous bulk.

Size Distribution of Solubilized Aggregates. The hydrodynamic diameters (d_H) of the aggregates in the solution with or without *n*-alkylbenzenes are plotted as a function of surfactant concentration in Figure 2. In the DLS results, there exists one maximum in size distribution over the entire concentration here, which indicates a monodisperse size distribution. The polydispersity index (PDI) of the present systems at the 2.0 mmol dm^{-3} 14-10-14,2Br$^-$ solution is in the range of 0.19 to 0.38 (288.2 K), 0.34 to 0.40 (298.2 K), and 0.21 to 0.38 (308.2 K). As seen in Figure 2, the d_H values for the micellar aggregate in the absence of *n*-alkylbenzenes is ∼5 nm at 2.0 mmol dm^{-3} 14-10-14,2Br$^-$ regardless of the temperature variation. The micellar aggregation number of 14-10-14,2Br$^-$ determined previously by the steady-state fluorescence quenching method is 11 ± 1 at 288.2−308.2 K.[34] On the other hand, the aggregates including the *n*-alkylbenzene becomes considerably larger in d_H. At 288.2 K (Figure 2A), the d_H values range roughly from 100 to 300 nm at 2.0 mmol dm^{-3} irrespective of the alkyl chain length of the solubilizates and become more than 20 times longer compared to that of the mother micelles just in water. The magnitude of the size growth of the aggregates becomes larger and larger with increasing temperatures: more than 50 times larger at 298.2 K (Figure 2B) and more than 80 times larger at 308.2 K (Figure 2C). These results provide the following findings: (i) the considerable growth in aggregate size is induced by

solubilization of the *n*-alkylbenzenes, (ii) 14-10-14,2Br$^-$ concentration above the cmc is less effective on the size of the aggregates, and (iii) higher temperatures bring about larger aggregate sizes. A typical cryo-TEM image of the 14-10-14,2Br$^-$ solution at 2.0 mmol dm^{-3} is shown in Figure 3. It indicates
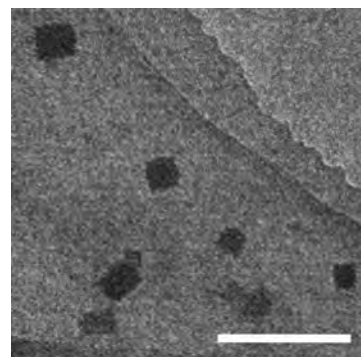
Figure 3. Cryo-TEM image of the 14-10-14,2Br$^-$ solution at 2.0 mmol dm^{-3}. The scale bar represents 500 nm.

several spheroidal or (vesicle-like) cubic micelles, which are seen as a dark contrast in the frame. The micelles have an average diameter of 95 ± 31 nm. The difference in diameter of the micelles between DLS and cryo-TEM is acceptable, if effects of the sample preparation for TEM observations are taken into account. Image observation for the 14-10-14,2Br$^-$ solution solubilized by *n*-butylbenzene has been performed to obtain information on the morphology of aggregates (data not shown). However, micrographs similar to Figure 3 were obtained because of the low melting point of *n*-butylbenzene (∼185 K) or its faster molecular motion during the solubilization process in surfactant micelles than the freezing velocity of the liquid component.

Gibbs Energy Change for Transfer. The size of micellar aggregates is found to be quite large from the DLS data. Thus, the partition equilibrium can be adopted to evaluate the Gibbs energy change (ΔG^0) for transfer of the solubilizate molecules from the aqueous bulk to the large aggregates. That is, the large molecular aggregate including the solubilizates can be regarded as a separate phase, if reasonable values for the Gibbs energy change are obtained by the partition equilibrium. The mole fractions of the solubilizates in the aqueous phase (X_R^W) and the aggregate phase (X_R^A) are given by eqs 2 and 3, respectively.

$$X_R^W = [R]/(55.5 + [R] + cmc) \tag{2}$$

$$X_R^A = ([R_t] - [R])/\{(C - cmc) + ([R_t] - [R])\} \quad (3)$$

where $[R_t]$ is the total equivalent concentration of the solubilizates and C is the total surfactant concentration. The subscript R refers to the solubilizate, and the superscripts W and A refer to the aqueous phase and the aggregate phase, respectively. The chemical potential of solubilizates in each phase is expressed as follows at temperature T and pressure P:

$$\mu_R^W = \mu_R^{\theta,W}(T, P) + RT \ln X_R^W \quad (4)$$

$$\mu_R^A = \mu_R^{0,A}(T, P + \Delta P) + RT \ln X_R^A \quad (5)$$

where ΔP is the difference in pressure between the aqueous and aggregate phases, μ^θ is the standard chemical potential at infinite dilution for the aqueous phase, and μ^0 is the standard chemical potential for the micellar phase based upon a symmetrically standardized state. It is noted that the concentration can be commonly substituted for activity in dilute surfactant systems. Accordingly, the following relationship is derived for the solubilizate molecules under equilibrium.

$$RT \ln(X_R^A/X_R^W) = -\{\mu_R^{0,A}(T, P + \Delta P) - \mu_R^{\theta,W}(T, P)\}$$
$$= -\Delta G^0 \quad (6)$$

The ΔG^0 values calculated from eq 6 are plotted against the number of carbon atoms in the alkyl chain of the solubilizates at different temperatures (Figure 4). The Gibbs energy change
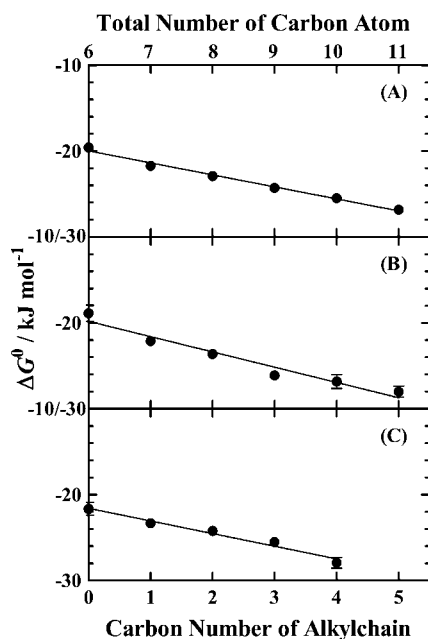
Figure 4. Gibbs energy change (ΔG^0) for solubilization against the carbon number of the alkyl chain of solubilizates at (A) 288.2, (B) 298.2, and (C) 308.2 K.

decreases almost linearly with increase in the alkyl chain length, which means that the solubilizates become more stabilized by solubilization with increasing alkyl chain length. In addition, the solubilization becomes favorable with increasing temperature. Unfortunately, the solubility of n-pentylbenzene in the surfactant solution at 308.2 K is too low to be measured precisely due to the limitations of the spectrophotometer. The contribution per methylene group of the alkyl chain to the Gibbs energy change ($\Delta G_{CH_2}^0$) is calculated to be -1.4 kJ mol^{-1}

at 288.2 K, -1.8 kJ mol^{-1} at 298.2 K, and -1.5 kJ mol^{-1} at 308.2 K from the slope in the figure. The value at 298.2 K is smaller in magnitude compared to that of -2.8 kJ mol^{-1} for the system of tetradecyltrimethylammoinum bromide (TTAB),[44] which is the monomer of 14-10-14,2Br$^-$. Therefore, it is made clear that n-alkylbenzenes become more difficult to solubilize into the inner core of 14-10-14,2Br$^-$ micelles than into that of TTAB micelles. These results imply that the spacer ($m = 10$) in 14-10-14,2Br$^-$ works as a hydrophilic moiety rather than as a hydrophobic one. Nevertheless, the $\Delta G_{CH_2}^0$ values indicate that the location of the alkyl chain of the solubilizates is a hydrophobic micellar core, which is also supported by the absorption spectrum (see the latter section).

From the variation of ΔG^0 vs temperature, the enthalpy and the entropy changes (ΔH^0 and ΔS^0) for solubilization can be evaluated by the following relations.

$$\Delta H^0 = \left[\frac{\partial(\Delta G^0/T)}{\partial(1/T)} \right]_p \quad (7)$$

$$-T\Delta S^0 = \Delta G^0 - \Delta H^0 \quad (8)$$

The variation of $\Delta G^0/T$ against $1/T$ is fitted with a first order approximation and the ΔH^0 value is subsequently estimated from the slope. The ΔH^0 and $-T\Delta S^0$ values are plotted as a function of carbon number in the alkyl chain of the solubilizates in Figure 5. The ΔG^0 value includes two terms of ΔH^0 and
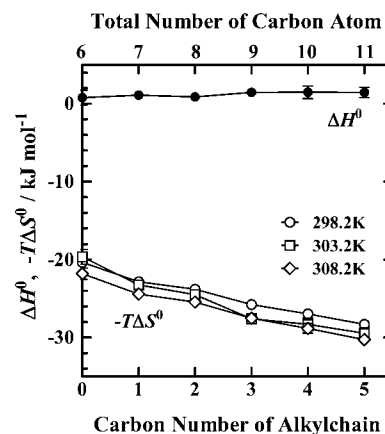

Figure 5. Enthalpy and the entropy changes for solubilization, ΔH^0 and $-T\Delta S^0$, against the carbon number of the alkyl chain of solubilizates at different temperatures.

$-T\Delta S^0$ as seen from eq 8. The ΔH^0 values are slightly positive and remain almost constant irrespective of the alkyl chain length of the solubilizates. On the other hand, the values of $-T\Delta S^0$ decrease almost linearly from -20 to -30 kJ mol^{-1} with increasing alkyl chain length. In addition, the values become more negative with increasing temperature. Therefore, it is made clear that the solubilization of n-alkylbenzenes into the 14-10-14,2Br$^-$ aggregates is driven by a positive entropy change, which results from the breakdown of structural water molecules around the alkyl chain of the solubilizates. The entropy-driven solubilization of the n-alkylbenzenes tends to be accomplished for the ionic surfactant systems.[10] On the other hand, as for the nonionic surfactant systems, the solubilization is driven by the negative enthalpy change, where the solubilizate molecules interact strongly with the surfactant.[6,7]
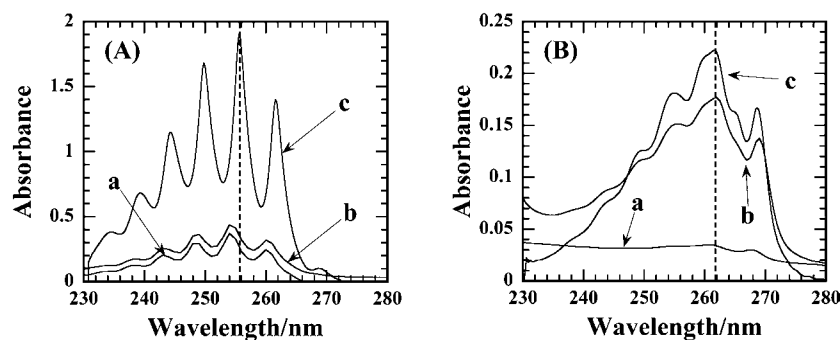
Figure 6. Absorption spectra of (A) benzene and (B) *n*-butylbenzene in 14-10-14,2Br⁻ aqueous solution (a) below the cmc, (b) above the cmc, and (c) in *n*-dodecane at 298.2 K. The wavelength of the highest peak of the spectrum in *n*-dodecane is indicated by a broken line.
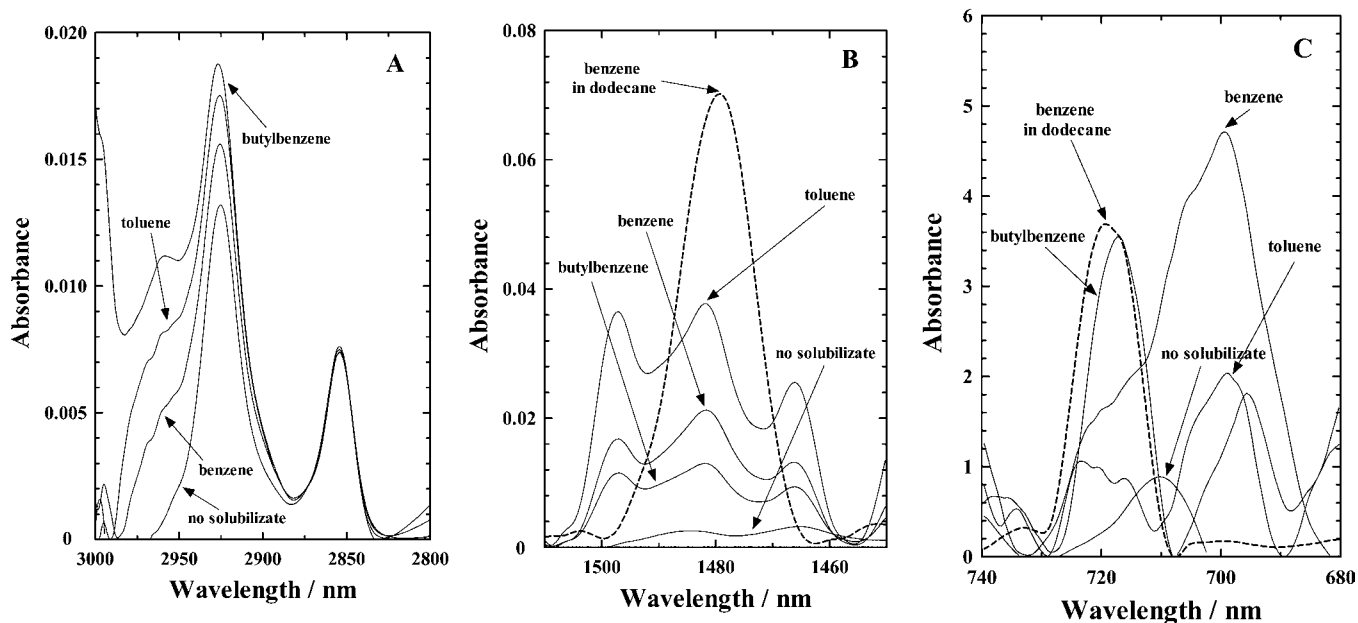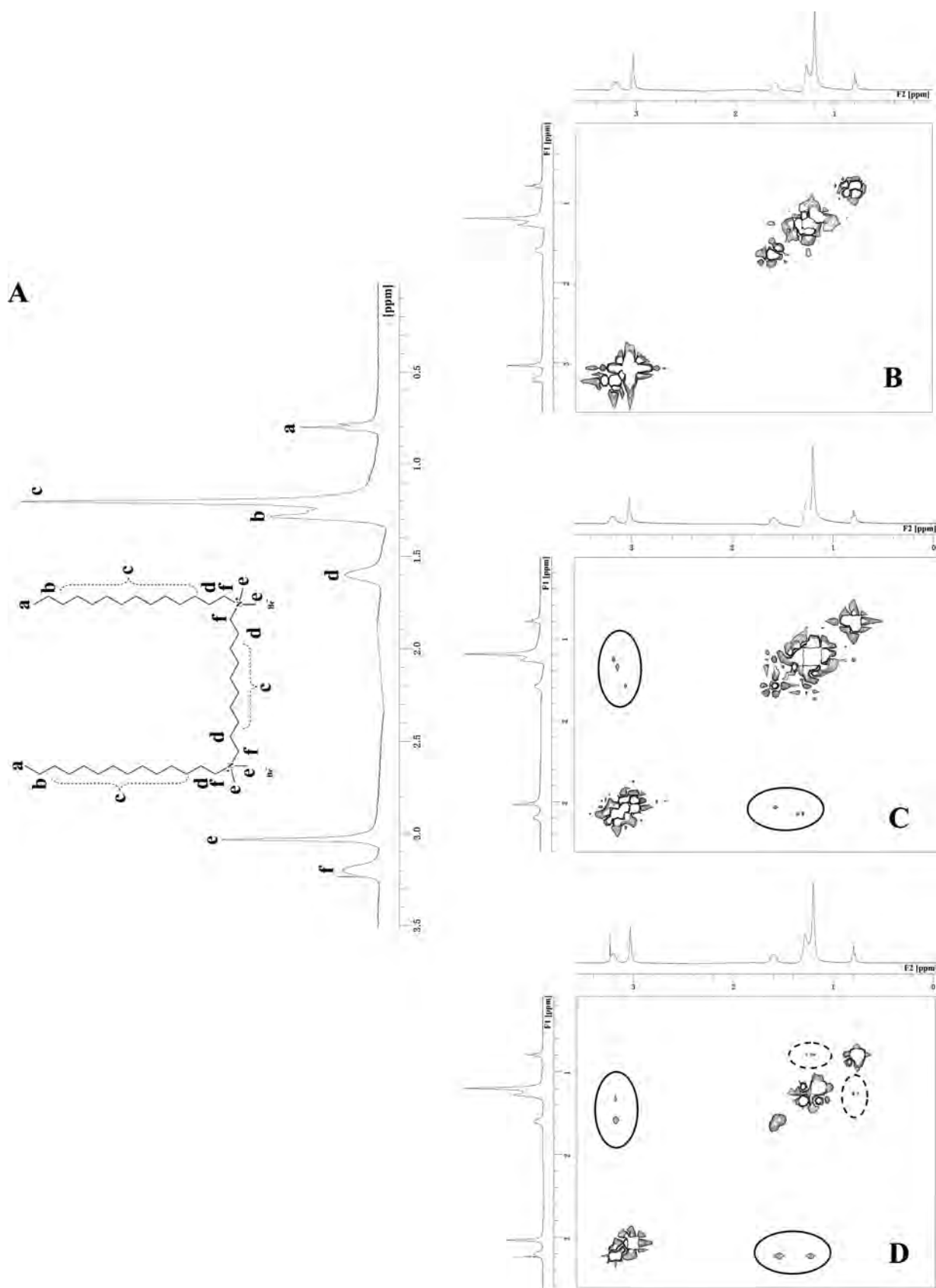

Figure 7. FTIR spectra of the 14-10-14,2Br⁻ solutions at 2.0 mmol dm⁻³ containing no solubilizates and solubilizing benzene, toluene, and *n*-butylbenzene in the region of (A) 2800−3000 cm⁻¹, (B) 1450−1510 cm⁻¹, and (C) 680−740 cm⁻¹. The broken lines represent the spectra of benzene in *n*-dodecane, where the intensity is an arbitrary unit.

That is, 14-10-14,2Br⁻ micelles are found to interact less with the *n*-alkylbenzenes than ionic micelles.

Absorption Spectrum of the Solubilizates. The representative absorption spectra of benzene and *n*-butylbenzene in the surfactant solution below and above the cmc are shown in Figure 6, where the spectra in *n*-dodecane are also traced together. The broken line in the figure indicates the wavelength at the highest peak in *n*-dodecane. As for the spectra of benzene in Figure 6A, the wavelengths of the highest peak below and above the cmc are identical to 254 nm. However, that of the spectrum in *n*-dodecane shifted to a higher wavelength of 256 nm. In common, the absorption spectrum of a molecule depends strongly on the dielectric constant of the environment where the molecules are located; the dielectric constant is 78.3 for water and 2.0 for *n*-dodecane at 298.2 K.[45] Hence, when the benzene ring of the *n*-alkylbenzenes is highly concentrated in the hydrophobic core of 14-10-14,2Br⁻ aggregates, the highest peak of the spectra should shift to the higher wavelength (the broken line). As a result, it is found from the above results that benzene molecules are located in the medium of relatively high dielectric constant made up of the headgroup and water molecules, not in the

hydrophobic micellar core. On the other hand, the spectrum of *n*-butylbenzene above the cmc shifts to a higher wavelength and is quite similar in peak position to that in *n*-dodecane (Figure 6B), which strongly indicates that the benzene ring is located in the more hydrophobic part of the micelle. These changes in spectrum have been observed for other surfactant systems.[6,7,44] Consequently, the spectrum shift above the cmc suggests that the solubilized *n*-alkylbenzene moves more into the inner core of the micelles with the elongation of the alkyl chain of the solubilizates.

FTIR Spectra of the Micellar Aggregates. The FTIR spectra in the region of 2800−3000 cm⁻¹ for the 14-10-14,2Br⁻ solutions in the absence and presence of benzene, toluene, and *n*-butylbenzene are shown in Figure 7A. The peaks observed in the region commonly catch stretching vibrations of methylene and methyl groups for amphiphiles. There are two major peaks such as a symmetric methylene stretching vibration (or $\nu_s(CH_2)$) at ∼2852 cm⁻¹ and an asymmetric methylene stretching vibration (or $\nu_a(CH_2)$) at ∼2924 cm⁻¹. Judging from the spectrum of the solution containing no solubilizates and the relatively small amounts of solubilizing *n*-alkylbenzenes in the 14-10-14,2Br⁻ solution, these peaks are found to be

Figure 8. (A) ^{1}H NMR spectrum of the 14-10-14,2Br$^-$ solutions at 2.0 mmol dm^{-3} at 298.2 K. 2-D NOESY maps for the 14-10-14,2Br$^-$ solutions at 2.0 mmol dm^{-3} containing (B) no solubilizates, (C) benzene, and (D) n-butylbenzene at 298.2 K.

mainly derived from hydrocarbon chains and spacer chains in a 14-10-14,2Br$^-$ molecule. The ν_a(CH$_2$) peak intensity increases

with extension of alkyl chain in solubilizates, although the ν_s(CH$_2$) mode indicates almost no variation in peak intensity.

That is, the relative ratio of peak intensities between $\nu_s(CH_2)$ and $\nu_a(CH_2)$ modes changes considerably depending on hydrophobicity of n-alkylbenzenes. This means that the solubilization of n-alkylbenzenes induces a fluctuation in the methylene vibration moment of 14-10-14,2Br$^-$ hydrophobic or spacer chains. Figure 7B shows the FTIR spectra in the region of 1450−1510 cm^{-1}, which reflects the vibration mode of benzene ring backbones. The spectrum for the 14-10-14,2Br$^-$ solution without solubilizates exhibits no major peaks. In contrast, the 14-10-14,2Br$^-$ solutions solubilizing n-alkylbenzenes indicate three kinds of absorption bands at 1466, 1482, and 1497 cm^{-1}. The first and third bands are assigned to methylene and methyl bending vibration, and benzene ring backbone mode (or C−C stretches in benzene ring), respectively. The second is assumed to be the benzene ring backbone mode in lipophilic environments because the band at ∼1479 cm^{-1} is observed for benzene in n-dodecane. These results support the evidence that n-alkylbenzenes are incorporated into the surfactant micelle. The region 680−740 cm^{-1} provides information on the C−H (out of plane) bending vibration in the benzene ring (see Figure 7C). The peak position of the C−H bending vibration is 699 cm^{-1} for benzene and toluene in the surfactant solution. On the other hand, the spectrum for n-butylbenzene in the solution exhibits two bands at ∼695 and ∼717 cm^{-1}. Considering the fact that the C−H band appears at ∼719 cm^{-1} for benzene in n-dodecane, it is thus found that the ∼695 and ∼717 cm^{-1} bands are reasonably assigned to the C−H modes located in the aqueous medium and inner micelle of the 14-10-14,2Br$^-$ solution, respectively. These FTIR spectra also support the above-mentioned transfer of solubilization sites into inner micelles with the elongation of alkyl chains in solubilizates.

2-D NOESY Plots. To complement the spectroscopic studies above, we have examined the internal structural change of the micelle induced by the solubilization of n-alkylbenzenes employing the two-dimensional nuclear Overhauser effect spectroscopy (2-D NOESY). This technique can provide detailed information on the spatial vicinity (<0.5 nm) of two different components and thus has been used as an effective method of studying the solubilization in micelles.[36,46] The ^{1}H NMR spectrum of the 14-10-14,2Br$^-$ solution at 2.0 mmol dm^{-3} is shown in Figure 8A, where the chemical structure of the surfactant is inserted. The characteristic peaks are assigned by labels a−f: (a) 0.80, (b) 1.28, (c) 1.20, (d) 1.60, (e) 3.03, and (f) 3.20 ppm.

The 2-D NOESY map of the 14-10-14,2Br$^-$ solution without solubilizates is shown in Figure 8B. Besides the diagonal peaks, there are no cross peaks between different protons in 14-10-14,2Br$^-$. This means loose conformation of hydrophobic chains and spacer chains in the micelles. As benzene is incorporated into the micelle (Figure 8C), three kinds of NOE peaks, which are indicated by circles, are observed as cross-peak sets c−f, d−f, and d−e, which indicate interactions between the methylene protons in the hydrocarbon or spacer chains and α-methylene protons, between α-methylene and β-methylene protons, and between α-methyl and β-methylene protons, respectively. As for the peak set c−f, in particular, the α-methylene protons are considered to possibly interact with the methylene protons in the spacer chains not in the hydrocarbon chains because of lack of the existence of the cross-peak sets such as b−c and a−c. These cross peaks suggest that the solubilized benzene is located near the hydrophilic moiety of the micelle, or the headgroup part. In the case of the solubilization of n-

butylbenzene (Figure 8D), the cross-peak set d−e disappears and the signal pairs of a−b and a−c, which are indicated by broken circles, are observed evidently. The proton interactions as described by cross-peaks a−b and a−c can be interpreted as the solubilization site of n-butylbenzene to be near the micelle core. According to the 2D-NOESY results, it is strongly suggested that the solubilization site moves from the curved interface to the hydrophobic core of the micelle with an increase in the alkyl chain length of the solubilizates. This finding agrees well with the results of absorption and FTIR spectrum measurements.

■ DISCUSSION

With the incorporation of solubilizates, the micellar aggregates in surfactant solutions often vary in size and form. The solubilization of solid solubilizates is, in common, induced by incorporation into the hydrophobic core of the mother micelles or the formation of mixed micelles with the surfactant. In the case of liquid solubilizates, the solubilized aggregate can be regarded as a thermodynamically stable O/W emulsion, where liquid solubilizates and solid surfactants correspond to an oil phase and an emulsifier, respectively. In both cases, the micellar aggregate undergoes a considerable change in size by the incorporation of solubilizates,[44] when the solubilized amount is pretty high. The size (in diameter) of solubilized aggregates including the n-alkylbenzenes in TTAB solutions ranges from 200 to 700 nm at 298.2 K.[44] In the present study, although the d_H value is different in nature from the diameter above, the distribution of the aggregate size (Figure 2B) is very close to that of the TTAB system. That is, both surfactants indicate the similar emulsifying effect for the solubilization of n-alkylbenzenes. However, considering the cmc (3.8 mmol dm^{-3}) of TTAB at 298.2 K,[44,47] the emulsifying effect of the 14-10-14,2Br$^-$ system is larger by 60 times or more than that of the TTAB system.

The thermodynamical analysis treated here is very important for understanding of the incorporation of solubilizates into surfactant aggregates. However, the degree (or quantitative information) of solubilization needs to be normalized in its application to the various fields mentioned in the Introduction section. Toward such applications, it is desirable in terms of solubilization efficacy that a larger amount of solubilizates can be dissolved in aqueous solutions at lower surfactant concentrations. Ozeki and Ikeda defined the solubilization power at the maximum additive concentration as $d[R_t]/d(C - cmc)$.[48] The index means the number of solubilized molecules per surfactant molecule comprising micelles. That is, the solubilization power depends strongly on the (quantitative) potential of micellization of surfactants, which is deeply related with the cmc. From Table 1, where the indices for benzene and toluene are not listed due to dissatisfaction at the maximum additive concentration in the present study, the solubilization

Table 1. Mean Solubilization Power (in mmol solubilizate/ mmol surfactant) for the n-Alkylbenzenes/14-10-14,2Br$^-$/ Water Systems

solubilizates	288.2 K	298.2 K	308.2 K
ethylbenzene	0.96	0.84	0.94
n-propylbenzene	0.62	0.60	0.63
n-butylbenzene	0.36	0.32	0.28
n-pentylbenzene	0.24	0.11	−

power decreases with elongation of the alkyl chain of the solubilizates. This results from the temperature dependence of the aqueous solubility of n-alkylbenzenes. The typical cationic surfactant systems solubilized by Sudan Red B show the solubilization power of $\sim 2 \times 10^{-3}$ at 298.2 K.[48,49] In the case of the sodium dodecyl sulfate (SDS) system, where pyrene has intruded, the index is reported to be $\sim 7 \times 10^{-3}$ at 298.2 K.[50] Thus, it is found that the 14-10-14,2Br⁻ solution is nearly 2 orders of magnitude larger in solubilization power than the conventional typical monomeric ionic surfactants. In the next step, we examine the power of nonionic surfactants, because they commonly show much lower cmc than ionic surfactants. The solution properties including solubilization for octaethylene glycol monotetradecyl ether ($C_{14}E_8$) have been extensively characterized.[6,51−53] The cmc of $C_{14}E_8$ at 298.2 K is ~ 0.018 mmol dm^{-3},[54] which is lower than that of 14-10-14,2Br⁻. In comparison to the present system, however, the solubilization power of the n-alkylbenzenes/$C_{14}E_8$/water system is slightly smaller than that of the present systems: 0.75 for ethylbenzene, 0.41 for n-propylbenzene, 0.19 for n-butylbenzene, and 0.096 for n-pentylbenzene at 298.2 K.[6] Thus, it can be said that 14-10-14,2Br⁻ is superior in solubilization efficacy to conventional ionic and nonionic surfactants. These specificities of 14-10-14,2Br⁻ are possibly brought about by the nature of spacers in gemini surfactants, because the solubilization power (0.01−0.03) of Sudan I for the cationic gemini surfactants containing ester bonds or hydroxyl groups is more than ten times lower.[32] However, it has not yet been thoroughly interpreted how the spacer plays an important role in the solubilization process. Nonetheless, it is notable that gemini surfactants have a high potential for practical use as a solubilizer.

CONCLUSION

The solubility of n-alkylbenzenes increases linearly with the 14-10-14,2Br⁻ concentration above the cmc. The Gibbs energy changes of solubilization decrease with increasing alkyl chain length of the solubilizates, where the micellar aggregates are supported to be separate phases. Therefore, the solubilizates for longer alkyl chains are found to be solubilized more easily into the micelles. The solubilized aggregates have hydrodynamic diameter of hundreds of micrometers and thus can be regarded as a thermodynamically stable emulsion. The enthalpy and entropy changes for solubilization indicate that the solubilization of n-alkylbenzenes into the 14-10-14,2Br⁻ aggregates is entropy-driven. Furthermore, it is suggested from the absorption spectrum shift above the cmc that the solubilization site moves into the inner core of the aggregates with increasing the alkyl chain lengths of the solubilizates. This finding is more directly supported by the peak shift of FTIR spectra and by the cross-peak change in 2-D NOESY maps. The solubilization power of the present system is larger by 2 orders of magnitude than those of the systems containing typical ionic surfactants. This would be a great advantage for small-scale use of surfactants.

ASSOCIATED CONTENT

Ⓢ Supporting Information

Description of solubilization concentrations at the other temperatures. This material is available free of charge via the Internet at http://pubs.acs.org.

AUTHOR INFORMATION

Corresponding Author
*Tel: +81-956-20-5686. Fax: +81-956-20-5686. E-mail: wosamu@niu.ac.jp. Website: http://www.niu.ac.jp/~pharm1/lab/physchem/indexenglish.html.

Notes
The authors declare no competing financial interest.

REFERENCES

(1) Moroi, Y. *Micelles: Theoretical and Applied Aspects*; Plenum Press: New York, 1992; Chapter 9, p 252.
(2) Elworthy, P. H.; Florence, A. T.; Macfarlane, C. B. *Solubilization by surface active agents and its application in chemistry and biological sciences*; Chapman & Hall: London, 1968.
(3) McBain, M. L. E.; Hutchinson, E. *Solubilization and related phenomena*; Academic Press: New York, 1955.
(4) Mitra, S.; Dungan, S. R. Cholesterol solubilization in aqueous micellar solutions of quillaja saponin, bile salts, or nonionic surfactants. *J. Agric. Food Chem.* **2000**, *49*, 384−394.
(5) Xiarchos, I.; Doulia, D. Effect of nonionic surfactants on the solubilization of alachlor. *J. Hazard. Mater.* **2006**, *136*, 882−888.
(6) Sato, Y.; Nakahara, H.; Moroi, Y.; Shibata, O. Solubilization of n-alkylbenzenes into octaethylene glycol mono-n-tetradecyl ether ($C_{14}E_8$) micelles. *Langmuir* **2007**, *23*, 7505−7509.
(7) Nakamura, S.; Kobayashi, L.; Tanaka, R.; Isoda-Yamashita, T.; Lee, J.; Moroi, Y. Solubilization of n-alkylbenzenes into decanoyl-N-methylglucamide (Mega-10) solution; temperature dependence. *Colloids Surf., B* **2009**, *69*, 135−140.
(8) Zheng, G.; Selvam, A.; Wong, J. W. C. Enhanced solubilization and desorption of organochlorine pesticides (OCPs) from soil by oil-swollen micelles formed with a nonionic surfactant. *Environ. Sci. Technol.* **2012**, *46*, 12062−12068.
(9) Alamiry, M. A. H.; Benniston, A. C.; Harriman, A. Effect of pressure on the solubilization of a fluorescent merocyanine dye by a nonionic surfactant. *J. Phys. Chem. B* **2012**, *116*, 253−260.
(10) Lee, J.; Moroi, Y. Solubilization of n-alkylbenzenes in aggregates of sodium dodecyl sulfate and a cationic polymer of high charge density (II). *Langmuir* **2004**, *20*, 6116−6119.
(11) Mehta, S. K.; Bhawna. Significant effect of polar head group of surfactants on the solubilization of Zein in mixed micellar (SDS-DDAB) media. *Colloids Surf., B* **2010**, *81*, 74−80.
(12) Mehta, S. K.; Chaudhary, S. Micropartioning and solubilization enhancement of 1,2-bis(bis(4-chlorophenyl) methyl)diselane in mixed micelles of binary and ternary cationic-nonionic surfactant mixtures. *Colloids Surf., B* **2011**, *83*, 139−147.
(13) Mehta, S. K.; Chaudhary, S.; Kumar, R.; Bhasin, K. K. Facile solubilization of organochalcogen compounds in mixed micelle formation of binary and ternary cationic-nonionic surfactant mixtures. *J. Phys. Chem. B* **2009**, *113*, 7188−7193.
(14) Rao, K. J.; Paria, S. Solubilization of naphthalene in the presence of plant-synthetic mixed surfactant systems. *J. Phys. Chem. B* **2008**, *113*, 474−481.
(15) Mehling, T.; Kloss, L.; Ingram, T.; Smirnova, I. Partition coefficients of ionizable solutes in mixed nonionic/ionic micellar systems. *Langmuir* **2013**, *29*, 1035−1044.
(16) Menger, F. M.; Littau, C. A. Gemini surfactants: a new class of self-assembling molecules. *J. Am. Chem. Soc.* **1993**, *115*, 10083−10090.

(17) Menger, F. M.; Littau, C. A. Gemini-surfactants: synthesis and properties. *J. Am. Chem. Soc.* **1991**, *113*, 1451−1452.

(18) Zana, R. Gemini (dimeric) surfactants. *Curr. Opin. Colloid Interface Sci.* **1996**, *1*, 566−571.

(19) Alami, E.; Levy, H.; Zana, R.; Skoulios, A. Alkanediyl-α,ω-bis(dimethylalkylammonium bromide) surfactants. 2. Structure of the lyotropic mesophases in the presence of water. *Langmuir* **1993**, *9*, 940−944.

(20) Alami, E.; Beinert, G.; Marie, P.; Zana, R. Alkanediyl-α,ω-bis(dimethylalkylammonium bromide) surfactants. 3. Behavior at the air-water interface. *Langmuir* **1993**, *9*, 1465−1467.

(21) Zana, R.; Benrraou, M.; Rueff, R. Alkanediyl-α,ω-bis-(dimethylalkylammonium bromide) surfactants. 1. Effect of the spacer chain length on the critical micelle concentration and micelle ionization degree. *Langmuir* **1991**, *7*, 1072−1075.

(22) Badea, I.; Verrall, R.; Baca-Estrada, M.; Tikoo, S.; Rosenberg, A.; Kumar, P.; Foldvari, M. In vivo cutaneous interferon-γ gene delivery using novel dicationic (gemini) surfactant−plasmid complexes. *J. Gene Med.* **2005**, *7*, 1200−1214.

(23) Chevalier, Y. New surfactants: new chemical functions and molecular architectures. *Curr. Opin. Colloid Interface Sci.* **2002**, *7*, 3−11.

(24) Kirby, A. J.; Camilleri, P.; Engberts, J. B. F. N.; Feiters, M. C.; Nolte, R. J. M.; Söderman, O.; Bergsma, M.; Bell, P. C.; Fielden, M. L.; García Rodríguez, C. L.; Guédat, P.; Kremer, A.; McGregor, C.; Perrin, C.; Ronsin, G.; van Eijk, M. C. P. Gemini surfactants: new synthetic vectors for gene transfection. *Angew. Chem., Int. Ed.* **2003**, *42*, 1448−1457.

(25) Rosenzweig, H. S.; Rakhmanova, V. A.; MacDonald, R. C. Diquaternary ammonium compounds as transfection agents. *Bioconjugate Chem.* **2001**, *12*, 258−263.

(26) Zana, R. Dimeric and oligomeric surfactants. Behavior at interfaces and in aqueous solution: a review. *Adv. Colloid Interface Sci.* **2002**, *97*, 205−253.

(27) Bernheim-Groswasser, A.; Zana, R.; Talmon, Y. Sphere-to-cylinder transition in aqueous micellar solution of a dimeric (gemini) surfactant. *J. Phys. Chem. B* **2000**, *104*, 4005−4009.

(28) Danino, D.; Talmon, Y.; Zana, R. Alkanediyl-α,ω-bis-(dimethylalkylammonium bromide) surfactants (dimeric surfactants). 5. Aggregation and microstructure in aqueous solutions. *Langmuir* **1995**, *11*, 1448−1456.

(29) Viscardi, G.; Quagliotto, P.; Barolo, C.; Savarino, P.; Barni, E.; Fisicaro, E. Synthesis and surface and antimicrobial properties of novel cationic surfactants. *J. Org. Chem.* **2000**, *65*, 8197−8203.

(30) Zana, R.; Talmon, Y. Dependence of aggregate morphology on structure of dimeric surfactants. *Nature* **1993**, *362*, 228−230.

(31) Zheng, O.; Zhao, J.-X. Solubilization of pyrene in aqueous micellar solutions of gemini surfactants C$_{12}$-s-C$_{12}$•2Br. *J. Colloid Interface Sci.* **2006**, *300*, 749−754.

(32) Tehrani-Bagha, A. R.; Singh, R. G.; Holmberg, K. Solubilization of two organic dyes by cationic ester-containing gemini surfactants. *J. Colloid Interface Sci.* **2012**, *376*, 112−118.

(33) Matsuoka, K.; Takeuchi, E.; Takahashi, M.; Kitsugi, S.; Honda, C.; Endo, K. Solubilization of n-alkylbenzene and n-perfluoroalkyl-benzene in hydrogenated and fluorinated surfactants micelles. *J. Colloid Interface Sci.* **2009**, *333*, 641−645.

(34) Nakahara, H.; Hasegawa, A.; Uehara, S.; Akisada, H.; Shibata, O. Solution properties of gemini surfactant of decanediyl-1-10-bis (dimethyltetradecylammonium bromide) in aqueous medium. *J. Oleo. Sci.* **2013**, *62*, 905−912.

(35) Chen, J.; Xue, H.; Yao, Y.; Yang, H.; Li, A.; Xu, M.; Chen, Q.; Cheng, R. Effect of surfactant concentration on the complex structure of poly(N-isopropylacrylamide)/sodium n-dodecyl sulfate in aqueous solutions. *Macromolecules* **2012**, *45*, 5524−5529.

(36) Padia, F. N.; Yaseen, M.; Gore, B.; Rogers, S.; Bell, G.; Lu, J. R. Influence of molecular structure on the size, shape, and nanostructure of nonionic C$_n$E$_m$ surfactant micelles. *J. Phys. Chem. B* **2014**, *118*, 179−188.

(37) Nakamura, S.; Kobayashi, L.; Tanaka, R.; Isoda-Yamashita, T.; Motomura, K.; Moroi, Y. Solubilization of n-alkylbenzenes into decanoyl-N-methylglucamide (Mega-10) solution. *Langmuir* **2008**, *24*, 15−18.

(38) Eastman, J. W.; Rehfeld, S. J. Interaction of the benzene molecule with liquid solvents. Fluorescence quenching parallels (0−0) ultraviolet absorption intensity. *J. Phys. Chem.* **1970**, *74*, 1438−1443.

(39) Take'uchi, M.; Moroi, Y. Solubilization of n-alkylbenzenes into 1-dodecanesulfonic acid micelles. *Langmuir* **1995**, *11*, 4719−4723.

(40) Take'uchi, M.; Moroi, Y. Solubilization of n-alkylbenzenes into lithium 1-perfluoroundecanoate micelles. *J. Colloid Interface Sci.* **1998**, *197*, 230−235.

(41) Tewari, Y. B.; Miller, M. M.; Wasik, S. P.; Martire, D. E. Aqueous solubility and octanol/water partition coefficient of organic compounds at 25.0 °C. *J. Chem. Eng. Data* **1982**, *27*, 451−454.

(42) Sanemasa, I.; Araki, M.; Deguchi, T.; Nagai, H. Solubility measurements of benzene and the alkylbenzenes in water by making use of solute vapor. *Bull. Chem. Soc. Jpn.* **1982**, *55*, 1054−1062.

(43) Myrdal, P.; Ward, G. H.; Dannenfelser, R.-M.; Mishra, D.; Yalkowsky, S. H. AQUAFAC 1: Aqueous functional group activity coefficients; application to hydrocarbons. *Chemosphere* **1992**, *24*, 1047−1061.

(44) Doi, Y.; Kawashima, Y.; Matsuoka, K.; Moroi, Y. O/W Emulsion of n-alkylbenzene/ionic surfactant/water systems. *J. Phys. Chem. B* **2004**, *108*, 2594−2599.

(45) Haynes, W. M. *CRC Handbook of Chemistry and Physics*, 91st ed.; CRC Press: Boca Raton, 2010; p 2610.

(46) McLachlan, A.; Singh, K.; Marangoni, D. G. A conformational investigation of zwitterionic surfactants in the micelle via ^{13}C chemical shift measurements and 2D NOESY spectroscopy. *Colloid Polym. Sci.* **2010**, *288*, 653−663.

(47) Aguiar, J.; J,A., M.-B.; Peula-García, J. M.; Carnero Ruiz, C. Thermodynamics and micellar properties of tetradecyltrimethylammonium bromide in formamide-water mixtures. *J. Colloid Interface Sci.* **2002**, *255*, 382−390.

(48) Ozeki, S.; Ikeda, S. The difference in solubilization power between spherical and rodlike micelles of dodecyldimethylammonium chloride in aqueous solutions. *J. Phys. Chem.* **1985**, *89*, 5088−5093.

(49) Ikeda, S.; Maruyama, Y. Solubilization of a water-insoluble dye in aqueous sodium halide solutions of dodecylpyridinium halides: effects of counterion species of ionic micelles. *J. Colloid Interface Sci.* **1994**, *166*, 1−5.

(50) Kim, J.-H.; Domach, M. M.; Tilton, R. D. Effect of electrolytes on the pyrene solubilization capacity of dodecyl sulfate micelles. *Langmuir* **2000**, *16*, 10037−10043.

(51) Kahlweit, M.; Busse, G.; Winkler, J. Electric conductivity in microemulsions. *J. Chem. Phys.* **1993**, *99*, 5605−5614.

(52) Yeh, M.-C.; Chen, L.-J. Wetting transitions at the air–liquid interface of water + tetradecane + C$_6$E$_2$ mixtures. *J. Chem. Phys.* **2001**, *115*, 8575−8582.

(53) Tamura, T.; Takeuchi, Y.; Kaneko, Y. Influence of surfactant structure on the drainage of nonionic surfactant foam films. *J. Colloid Interface Sci.* **1998**, *206*, 112−121.

(54) Rusdi, M.; Moroi, Y.; Hlaing, T.; Matsuoka, K. Micelle formation and surface adsorption of octaethylene glycol monoalkyl ether (C$_n$E$_8$). *Bull. Chem. Soc. Jpn.* **2005**, *78*, 604−610.